Renewable and Sustainable Energy Reviews 151 (2021) 111621

Contents lists available at ScienceDirect

Renewable and Sustainable Energy Reviews

journal homepage: www.elsevier.com/locate/rser

Analysis of global energy savings in the frozen food industry made possible by transitioning from conventional isobaric freezing to isochoric freezing

Yuanheng Zhao [a,b,c,1], Matthew J. Powell-Palm [b,1], Junjie Wang [a], Cristina Bilbao-Sainz [d], Tara McHugh [d], Boris Rubinsky [b,*]

[a] Chinese Academy of Sciences Key Laboratory of Cryogenics, Technical Institute of Physics and Chemistry, Beijing, 100190, China
[b] Department of Mechanical Engineering, University of California at Berkeley, Berkeley, CA, 94720, USA
[c] University of Chinese Academy of Sciences, Beijing, 100049, China
[d] Western Regional Research Center, US Department of Agriculture, Albany, CA, 94710, USA

ARTICLE INFO

Keywords:
Isochoric freezing
Isochoric supercooling
Energy savings
Frozen food
Cold storage
Global cold-chain

ABSTRACT

An efficient global cold food chain is critical to the sustainability of the growing world population, and it is anticipated that the global frozen food market will reach $404.8 billion by 2027. Frozen foods are typically stored under conventional industry-standard isobaric (constant-pressure) conditions at sub-freezing temperatures, however, which can degrade the textural and nutritional quality of the food and comes at high energetic and carbon costs. While efforts to reduce this energetic toll have traditionally targeted the devices used to generate refrigeration, we herein identify that significant energy savings may be attainable by altering the fundamental thermodynamics of the freezing process itself. Here we show that preserving frozen food under isochoric (constant-volume) thermodynamic conditions, as opposed to conventional isobaric conditions, may theoretically reduce annual global energy consumption by as much as 6.49 billion kWh, with accompanying carbon emission savings of 4.59 billion kg. Importantly, these savings can be achieved rapidly and inexpensively, without any costly changes to the current global refrigeration infrastructure. Furthermore, early studies demonstrate that isochoric freezing results in substantially improved food quality, extends the preservable lifetime of fresh and otherwise delicate food products, and has cross-cutting biopreservation applications in domains as diverse as medicine, biology, and pharmaceuticals.

1. Introduction

The development of sustainable, equitable, and inclusive global food chains in the face of a growing population represents a landmark challenge on the path towards global sustainability in the 21st century. Meeting this challenge will require innovation in multiples domains, but perhaps most pressingly in the food cold-chain. Cold storage of food is integral to global food capacitance (i.e. the ability to store and distribute food resources as necessary). Its efficacy and availability have huge implications on global food waste (which has been estimated at greater than 30% of total post-harvest yields) [1–3], safety [4], and accessibility. Estimates anticipate a continuous growth in the frozen food market, from $291.8 billion in 2019 to $404.8 billion in 2027 [5].

The current global cold-chain operates at significant energetic costs; domestic food cold-storage alone was estimated to account for nearly 4% of all global electricity consumption annually [6], equivalent to 6.54×10^8 metric tons of emitted carbon dioxide [7] and costing approximately 120 billion USD. The high economic and climatological price of essential cold-storage infrastructure creates systemic inequalities in food access between countries with high- and low-income economies. Thus, in envisioning an energy efficient future food chain, capable of meeting the needs of a soaring global population, fundamental innovations in the cold-storage space are needed to reduce both the economic burden, the energetic burden and the carbon footprint of the cold-storage infrastructure.

Cold storage of food is driven by the strong temperature dependence of metabolism. Lowering the temperature reduces the metabolism, thereby slowing the deterioration of food and the growth of contaminant microorganisms. However, in an isobaric (constant-pressure) thermodynamic environment open to the atmosphere (as virtually all modern food storage presently is), food matter (being comprised largely of

* Corresponding author.
E-mail address: rubinsky@berkeley.edu (B. Rubinsky).
[1] Matthew Powell-Palm and Yuanheng Zhao made equal first authorship contributions to this study.

https://doi.org/10.1016/j.rser.2021.111621
Received 10 March 2021; Received in revised form 23 July 2021; Accepted 27 August 2021

Nomenclature

C	Carbon emissions (CO_2), [kg]
$c_p(T)$	Isobaric specific heat capacity, [J/(kg•°C)]
$c_v(T)$	Isochoric specific heat capacity, [J/(kg•°C)]
COP	Coefficient of performance of the refrigerator/freezer
$COST$	Cost of electricity consumed by the refrigerator/freezer, [USD]
E	Total energy expended per unit mass of food product, $\left[\frac{J}{kg}\right]$
H	Latent heat of phase change from water to ice, [kJ/kg]
h	Convection coefficient of chilled air within freezer cabinet, $[\frac{W}{m^2 \cdot C}]$
k	Thermal conductivity of the food product, [W/(m•°C)]
L	Half-length of 1D domain representing the food mass, [m]
m	Mass of stored food, [kg]
P	Hydrostatic pressure that develops in an isochoric system, [MPa]
T	Temperature of the food product, [°C]
T_0	Initial temperature, [°C]
T_f	Phase transition temperature, [°C]
$T_f(\phi)$	Freezing point of physiological saline solution as a function of ice fraction in isochoric systems, [°C]
t	Run time of the compressor in the freezer, [s]
W	Electrical work consumed by freezer, [kWh]
$\delta(t)$	Time-dependent position of the phase transition interface, [m]
ρ	Density of the specimen, [kg/m^3]
α	Thermal diffusivity of physiological saline in the isochoric system, [m^2/s]

Subscripts

freeze	Pertaining to the initial freezing/cooling process
storage	Pertaining to the extended cold storage process
isobaric	Isobaric conditions
isochoric	Isochoric conditions
l	Pertaining to the liquid phase
s	Pertaining to the solid phase

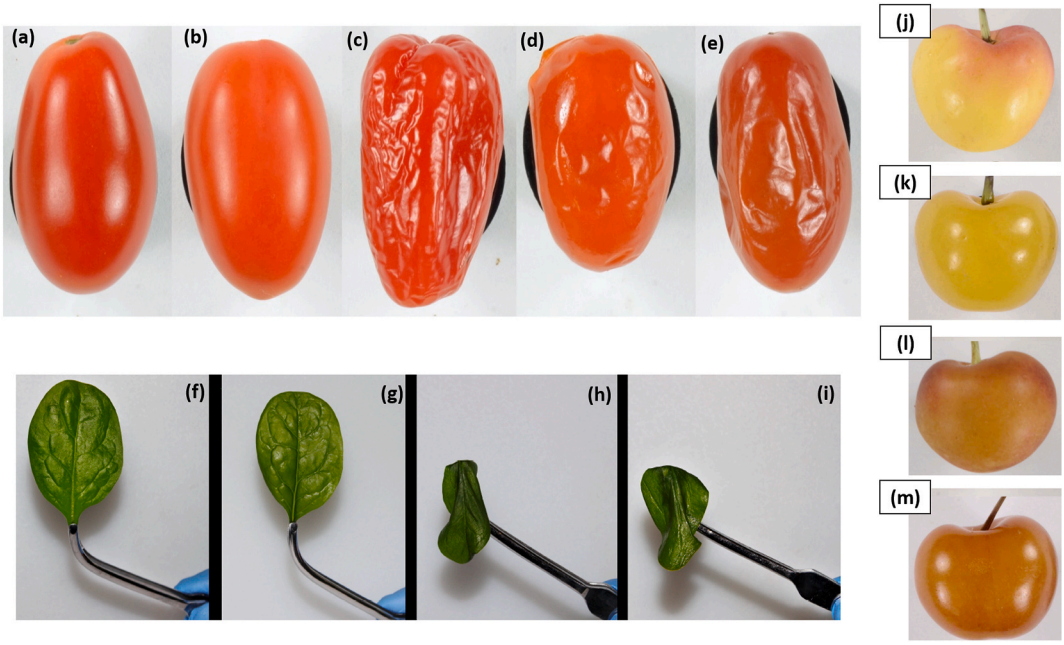

Fig. 1. Comparison between isochoric cold storage and conventional isobaric storage. **(a) to (e)** [27]. Fresh tomatoes stored four weeks: (**a**) fresh controls, (**b**) isochoric storage at −2.5 °C, (**c**) conventional refrigerator storage at 10 °C and 85% relative humidity, (**d**) conventional flash freezing and refrigeration storage at −20 °C, (**e**) isobaric storage at −2.5 °C. **(f) to (i)** [28]. Fresh spinach stored for one week: (**f**) fresh controls, (**g**) isochoric storage at −4 °C, (**h**) isobaric storage at −4 °C, (**i**) commercial, flash freezing and freezing storage at −20 °C. **(j) to (m)** [30]. Fresh cherries stored for 24 h: (**j**) fresh controls, (**k**) isochoric at −7 °C, (**l**) isobaric at −7 °C, (**m**) conventional liquid nitrogen freezing and refrigeration storage at −20 °C. (Figures modified from the listed references).

water), will freeze at sub 0 °C temperatures. The ice crystals that form upon freezing can substantially degrade the textural and nutritional quality of the food, and the central efforts of the modern food cold storage community seek to ameliorate the deleterious effects of these ice crystals while preserving the beneficial effects of low-temperature preservation, e.g. Refs. [8,9]. Quick freezing, which can decrease the size of ice crystals and thereby reduce morphological damage to frozen foods, revolutionized the food industry in the early 20th century [10] and is still today considered the gold standard of frozen storage [11,12]. The rapid cooling methods that are commonly used in the food industry are: a) freezing to liquid nitrogen temperatures (−196 °C), b) freezing to −100 °C, c) freezing to −40 °C and d) hyperbaric freezing in which the pressure of the system is first increased (an energy consuming process) and then suddenly released [13,14]. Maintaining these ultra-low temperatures at which food is rapidly frozen during subsequent continuous storage is extremely energy-intensive and requires specialized refrigeration systems. Therefore frozen food is typically stored at substantially higher temperatures than those at which it is initially frozen. However, this transition in storage temperatures can also lead to food damage, due to such mechanisms as ice recrystallization and fluid migration [15]. Therefore, in the cold food chain, a balance is sought between temperatures low enough to reduce recrystallization and temperatures at which

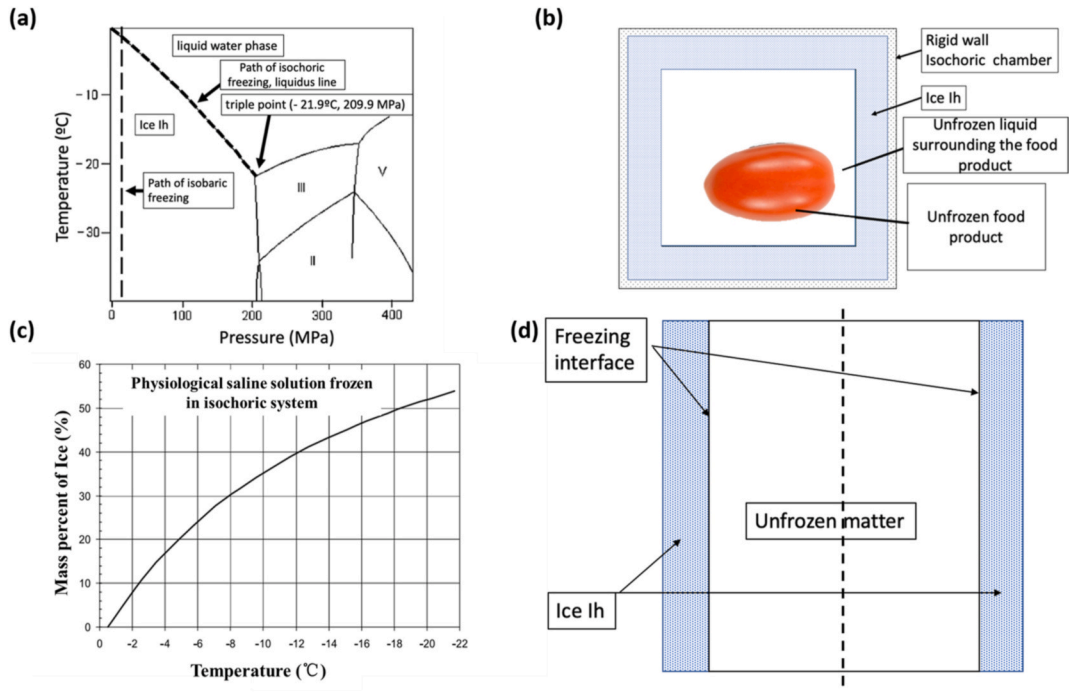

Fig. 2. Isochoric freezing thermodynamics and design. (a) Ice-water phase diagram showing an isochoric and isobaric freezing process. **(b)** Schematic of isochoric preservation of food (physiological saline solution) at subfreezing temperatures. **(c)** Mass percentage of ice that forms and the according equilibrium pressure in an isochoric system of ice and water. **(d)** Schematic representation of the freezing slab like configuration used to analyze an isochoric system in this work. The equivalent isobaric domain is subject to the same boundary conditions but contains no interior phase change interface, as at subfreezing temperatures the entire domain becomes ice.

the energy costs are acceptable. Most commercial cold storage systems use storage temperatures between −10 °C and −18 °C. In order to attain energy savings in the cold storage domain, many contemporary research efforts aim to re-examine the technological methods by which we generate this cold, from improving the efficiency of conventional vapor-compression freezers [16–18], to conceiving new refrigeration processes based on novel thermodynamic principles [18]. However, little research by comparison has questioned the fundamental thermodynamics at play within the freezing food matter itself, and the potential energy-saving benefits of extreme departures from conventional frozen storage.

Building from fundamental thermodynamic principles, we have developed a new concept for food storage at subfreezing temperatures, "isochoric cold storage" [19]. This storage modality aims to replace industry-standard cold storage, which occurs under constant atmospheric pressure (isobaric) conditions, with cold storage that instead occurs in constant volume (isochoric) conditions. Superficially, the difference between isobaric and isochoric systems appears minor: an isobaric container (volume) is open to the atmosphere (which functions as a pressure reservoir), while an isochoric container (volume) is closed to the atmosphere. However, thermodynamic theory and experiment show that the isochoric process of cold storage is profoundly different from its isobaric equivalent [19–24] resulting in substantial improvements in the quality of the preserved food [25,26]. Furthermore, isochoric systems can be used for storing foods that are otherwise difficult to preserve with isobaric freezing, such as tomatoes [27], spinach [28], cut potatoes [29], sweet cherries [30], etc. For example, isochoric preservation of tomatoes for one month led to improved quality stability of tomato fruits when compared with conventional preservation techniques such as individual quick freezing (IQF) [27]. Tomatoes preserved at −2.5 °C in an isochoric system showed the most desirable sensory characteristics in terms of mass, shape, volume, color and texture retention, and retained 98% ascorbic acid, 98% lycopene, 88% phenolic compound and 94% antioxidant activity. In comparison, ice formation during IQF freezing led to 17% mass loss and 16% volume loss, which contributed changes to both overall visual quality and firmness and reduced nutrient retention, (87% ascorbic acid, 33% lycopene, 40% phenolic compounds and 36% antioxidant activity). In another recent study, cut raw potatoes preserved at −3 °C for one month under isochoric conditions had lower drip loss and volume shrinkage as well as better preserved texture and microstructure than cut raw potatoes conventionally preserved at atmospheric pressures [29]. Finally, the potential of isochoric freezing for the development of value-added products and processes has also recently been demonstrated: value-added food products with improved nutrition and functionality can be produced using the enhanced hydrostatic pressures generated during isochoric freezing, which allow the infusion of bioactive compounds such as nutritional compounds, anti-browning agents, firming agents, antimicrobials, etc. into foods [31]; and processes that combine food storage and food safety measures can be developed by leveraging the unique bacterial sterilization effects observed in isochoric systems at low temperatures [32,33].

Illustrative examples comparing isochoric and isobaric storage of sensitive foods are shown in Fig. 1. Our results in these papers show that optimal isochoric storage temperatures are between −2.5 °C and −7 °C. The ability to cold-store these difficult-to-freeze products can have a major effect on world-wide reduction of food waste efforts.

It should also be noted that the process of isochoric freezing is not limited to the food domain, but is in fact applicable to issues of biological preservation in domains as divergent as medicine, conservation biology, and space travel. Notable recent efforts have employed isochoric freezing in the global effort to preserve complex organs and tissues outside the body for transplant [34,35], demonstrating the first-ever preservation of full mammalian hearts at sub-zero centigrade temperatures without chemical cryoprotectants [36], the first-ever multiday preservation of autonomously beating genetically-human engineered cardiac tissue [37], and successful multiday preservation of mammalian pancreatic islets [38].

Table 1
Thermodynamic data.

(a) Thermodynamic Storage Modes		(b) COP of Vapor-Compression Freezer	
Thermodynamic Storage Mode	Operating Temperatures (°C)	Coefficient of Performance (COP)	Operating Temperature (°C)
Isochoric Freezing	[−2.5, −5, −10, −18]	4.41	−2.5
Isochoric Supercooling	[−2.5, −5, −10]	4.1	−5
Isobaric Freezing	[−2.5, −5, −10, −18, −40, −100, −196]	3.53	−10
Hyperbaric Freezing	[−18]	3.06	−15
		2.86	−18

While these attributes of isochoric cold storage are all of value to the global food economy and health, the primary motivation for this work comes from a distinct and nuanced thermodynamic finding: In addition to improvements in the quality and safety of the cold stored food, isochoric cold storage consumes substantially less energy than isobaric cold storage [39,40].

The process of freezing in an isochoric system can be explained in thermodynamic terms by application of Le Chatelier's principle or analysis of Helmholtz free energies of water and ice [22,23]. From a high-level physical viewpoint, however, the unique behaviors experienced in isochoric systems can be thought of as a result of the expansion undergone by liquid water in transitioning to ice-Ih, which has a lower density than water. If water is confined within a constant-volume container, as freezing initiates, the lower-density ice Ih cannot freely expand, and it thus compresses the yet-unfrozen portion of the liquid, forcing the freezing process to proceed along the "liquidus line" of the Temperature-Pressure phase diagram. Fig. 2a illustrates the thermodynamic path that isochoric freezing takes (as an ice-water two-phase mixture along the liquidus line) alongside the isobaric freezing path (in which the entire system will freeze after the marked constant pressure line intersects the liquidus line in temperature). Fig. 2b shows that at −18 °C (the industry-standard frozen storage temperature), less than 50% of an isochoric volume will freeze. This of course suggests the possibility that food matter can be preserved in the remaining liquid phase of the isochoric system at subfreezing temperatures in an unfrozen state, and therefore, without concern for the effects of ice crystals on the quality of the food and without the need to resort to complex and energy-intensive cold storage protocols such as quick freezing. An illustration of the concept of isochoric freezing is shown in Fig. 2c.

It is important to emphasize in advance that refurbishing the global "isobaric" cold storage food chain with "isochoric" storage does not require any substantial changes in global refrigeration infrastructure, as it is a mode of storing food *within* a refrigeration system, and thus avoids the economic and logistical specter of replacing the billions of domestic and industrial refrigeration units currently in use. Isochoric cold storage simply replaces conventional storage containers with sealed, constant-volume containers; it is not dependent on any specific means of refrigeration, and thus may also be seamlessly integrated with both current conventional infrastructure and any novel refrigeration systems that may achieve widespread use in the future. For completeness, we also mention another thermodynamic food storage method that is less common, supercooling, in which the food mass is cooled only mildly past the freezing point and held in a metastable ice-free liquid state [24,34]. This form of cooling also exists in isobaric and isochoric variants, and we have recently demonstrated through thermodynamic analysis and experiments that supercooling under isochoric conditions is substantially more stable than supercooling under isobaric conditions. It is important to emphasize here, that in isochoric cold storage, either through freezing or supercooling, the processing and storage considerations which have conventionally constrained isobaric cold storage due to considerations of ice-related damage simply do not apply. Isobaric and hyperbaric freezing results in ice crystal formation, driving substantial degradation of the textural and nutritional quality of the food [13–15]; isochoric storage modes (freezing/supercooling) preserve food without ice damage [27–30,37], resulting in improved quality. Therefore, while for isobaric cold storage there is a strong argument for storing frozen foods at −18 °C to avoid secondary affects related to ice formation (such as recrystallization), in isochoric storage any optimal subfreezing temperature can be used.

In this work, we analyze the energy savings, reduction in global energy burden, and reduction in carbon footprint that could be accrued from transitioning the global food cold chain from isobaric cold storage to isochoric cold storage. We develop a simple two-part phase change model to describe the thermodynamics of frozen food storage in several thermodynamic storage modes: traditional isobaric freezing; hyperbaric (or pressure-shift) freezing [13,14]; isochoric freezing, and isochoric supercooling [24], which we evaluate at several storage temperatures reflecting various processes found in the industry. The Methodology section of this paper describes the mathematical model and calculations used to compare the energy expenditure for cold storage in isochoric systems and various isobaric systems.

2. Methodology

2.1. Thermodynamic model

We developed a simple two-part phase change model to describe the thermodynamics of frozen food storage in several thermodynamic storage modes: traditional isobaric freezing; hyperbaric (or pressure-shift) freezing [13,14]; isochoric freezing, and isochoric supercooling [24], which we evaluate at several storage temperatures reflecting various processes found in the industry. These thermodynamic regimes are summarized in Table 1a. Nomenclature and relevant units for all thermophysical properties and relations employed can be found in the *Nomenclature Table* and Supplementary information (SI).

Our model treats the two thermodynamically significant portions of the food cold-storage process: initial freezing and extended storage. Throughout the model, an arbitrary mass m of food is considered, which for the purpose of simplicity is modeled as a mass of physiological (0.09%) saline solution with a freezing point of $T_f = -0.56$ °C. For isobaric conditions, this food mass m comprises the total mass of the thermodynamic system. In order to calculate the temperature history and energy required during freezing and storage, the heat transfer problem is required to be solved. Here, the governing equations for each thermodynamic case are provided as follows. In all cases, a simple finite difference scheme is used to solve the equations. Standard mesh halving was employed to verify solution convergence. In reproducing these results, any chosen method of solving the following equations should prove sufficient.

2.1.1. Isochoric freezing

During isochoric freezing and storage, food products are immersed in liquid in a rigid constant-volume chamber [19]. Ice begins to expand when the chamber interior reaches sub-0°C temperatures, generating a hydrostatic pressure which in turn prevents further ice formation and results in a stable two-phase, liquid-ice equilibrium [19–24], wherein food products are stored in the liquid portion and thereby protected from any form of ice-related damage. Accordingly, only a limited portion of an isochoric system actually freezes (along the exterior closest to the cold source), and thus the system will always feature a frozen (subscript s) and unfrozen (subscript l) region and a phase-change interface between them, as shown in Fig. 2d. The time-dependent position of the interface is denoted by $\delta(t)$.

The energy for the frozen region is given by:

$$\frac{\partial T_s}{\partial t} = \alpha_s \frac{\partial^2 T_s}{\partial x_s^2},\ 0 \le x \le \delta(t) and\ t > 0 \tag{1}$$

The energy balance for the unfrozen region is given by:

$$\frac{\partial T_s}{\partial t} = \alpha_s \frac{\partial^2 T_s}{\partial x_s^2},\ \delta(t) \le x \le L_{isochoric}\ and\ t > 0 \tag{2}$$

The coupling conditions at the interface are:

$$k_s \frac{\partial T_s}{\partial x_s}|_{x=\delta} - k_l \frac{\partial T_l}{\partial x_l}|_{x=\delta} = \rho_l \cdot H_\delta \frac{\partial \delta}{\partial t}, \quad x = \delta(t) \tag{3}$$

$$T_s(x=\delta(t),t) = T_l(x=\delta(t),t) = T_f(\delta) \tag{4}$$

H_δ represents the constant volume latent heat of fusion, which is evaluated according to the following relation [41]:

$$H_\delta = 1.62 \times 10^{-4} T_{ph}^4 + 5.51 \times 10^{-3} T_{ph}^3 + 7.94 \times 10^{-2} T_{ph}^2 + 5.29 T_{ph} + 3.34 \times 10^2 \tag{5}$$

The phase change interface temperature varies with the ice percent in the isochoric system, which can be obtained from Fig. 2c as $T(\delta(t)) = T_{ph}(IPm)$. The correlation between the change in phase transition temperature $T_{ph}(IPm)$ as a result of ice percent (in mass) IPm for physiological saline solution, is given by [19].

$$T_{ph}(IPm) = -7 \times 10^{-5} IPm^3 - 2 \times 10^{-4} IPm^2 - 1.94 \times 10^{-1} IPm - 0.56 \tag{6}$$

where $T(IPm)$ is in °C and IPm is in 0–1.

The pressure (MPa) increases with the increase in mass fraction of ice according to the following relation from [41].

$$P = 8.78 \times 10^2 IPm^4 + 2.75 \times 10^2 IPm^3 + 3.24 \times 10^2 IPm^2 + 1.97 \times 10^2 IPm + 0.31 \tag{7}$$

In isochoric freezing/storage processes, two different configurations are considered, reflecting different use cases. In configuration 1, applicable to isochoric storage of juices and other liquid products, pre-frozen meals, or any other food product in which ice formation is deemed acceptable, the isochoric system mass is identical to the isobaric equivalent ($m_{isochoric} = m$) and limited ice formation is allowed to occur within the food mass:

$$L_{isochoric} = L\ (Configuration\ 1) \tag{8}$$

In configuration 2, which represents most isochoric food preservation research to date, sensitive food materials such as fresh fruits and vegetables may be stored in the portion of the system that remains liquid at sub-freezing temperatures, guaranteeing protection from ice damage. Accordingly, the isochoric system is sized to ensure that the food mass remains unfrozen and that there is sufficient excess solution to allow restricted ice formation at the exterior of the system, as shown conceptually in Fig. 2b and c. To account for this aspect, we employ a modified mass $m_{isochoric} = m/(1 - \phi(T_{storage}))$, that is

$$L_{isochoric} = L \,/\, \left(1 - \phi\left(T_{storage}\right)\right)\ (Configuration\ 2) \tag{9}$$

wherein $\phi(T_{storage})$ is the fraction of the isochoric system contents that will freeze at a given storage temperature per Fig. 2c.

2.1.2. Isobaric freezing

Conventionally, food products are frozen in an isobaric (constant-pressure) environment open to the atmosphere, e.g. food samples placed directly in a refrigerator [8,9]. The isobaric domain is divided into two parts: cooling with phase-change (while the domain is still freezing) and frozen cooling/storage (when the domain has frozen completely).

2.1.2. a For cooling with phase change ($T(x = L) \ge -0.56°C$), the domain is a 1D half-space geometrically identical to Fig. 2d, with a moving phase change interface. The governing equations are the same as Eqns. (1)–(3).

The coupling conditions at the interface is:

$$T_s(x = \delta(t), t) = -0.56°C \tag{10}$$

2.1.2. b For frozen cooling ($T(x = L) < -0.56°C$), there is no phase change and no moving phase interface.

The energy balance for the entire domain is thus given by:

$$\frac{\partial T_s}{\partial t} = \alpha_s \frac{\partial^2 T_s}{\partial x_s^2}\ 0 \le x \le L\ and\ t > 0 \tag{11}$$

2.1.3. Isochoric supercooling

During isochoric supercooling, food samples are immersed in liquid in a rigid constant-volume chamber (there is no air inside the chamber and the liquid is isolated from the atmosphere), which is then reduced in temperature only a few degrees past the freezing point of the liquid. At these mild sub-freezing temperatures, there are insufficient kinetic stimuli to nucleate ice crystals [22,24], and the system will remain in a metastable, supercooled, unfrozen state [37]. Supercooled storage keeps the entire domain unfrozen:

$$\frac{\partial T_l}{\partial t} = \alpha_l \frac{\partial^2 T_l}{\partial x_l^2}, \quad 0 \le x \le L\ and\ t > 0 \tag{12}$$

2.2. Initial cooling/freezing

2.2.1. Temperature history during cooling/freezing

In order to estimate the energy, E_{freeze}, required for initial freezing, the latent heat expenditure required to freeze the food mass at its freezing point T_f and the sensible heat required to cool the mass from an initial temperature $T_0 = 20°C$ to the target storage temperatures $T_{storage}$ presented in Table 1a must be summed. It should be noted however that the compressor is assumed to be running continuously during the initial cooling/freezing step, and the desired storage temperature $T_{storage}$ is constant (corresponding value is shown in Table 1a).

To calculate the temperature during the initial cooling/freezing process, the following initial condition is provided as:

$$T(x, t=0) = T_0 = 20°C\ ,\ at\ t = 0 \tag{13}$$

and the following boundary conditions:

$$h\left(T_{storage} - T_{surface}\right) = k_s \frac{\partial T}{\partial x}|_{x=0},\ at\ x = 0,\ t > 0 \tag{14}$$

$$\frac{\partial T}{\partial x}|_{x=L} = 0\ at\ x = L,\ t > 0 \tag{15}$$

Eqns. 1–15 are solved using MATLAB software to obtain the temperature profile for the initial cooling and freezing process in the case of isobaric and isochoric freezing. A variant front-tracking method is used which employs a fixed Δx advancement of the interface and solves for the according time needed for that advancement Δt. This method is commonplace for standard isobaric solidification, and the modifications made to accommodate isochoric conditions are described in our previous work [42]. Use of a fixed- Δx method allows for the initial cooling process preceding advancement of the phase change interface (e.g. the period during which the first node of the domain cools from room temperature to the freezing point) to be captured in the first Δt node (which will be large as a result). For isochoric supercooling, which involves no phase change, the temperature evolution of the system is time in trivial, and can be found using any standard analytical solution or numerical scheme for a slab subject to the boundary conditions described.

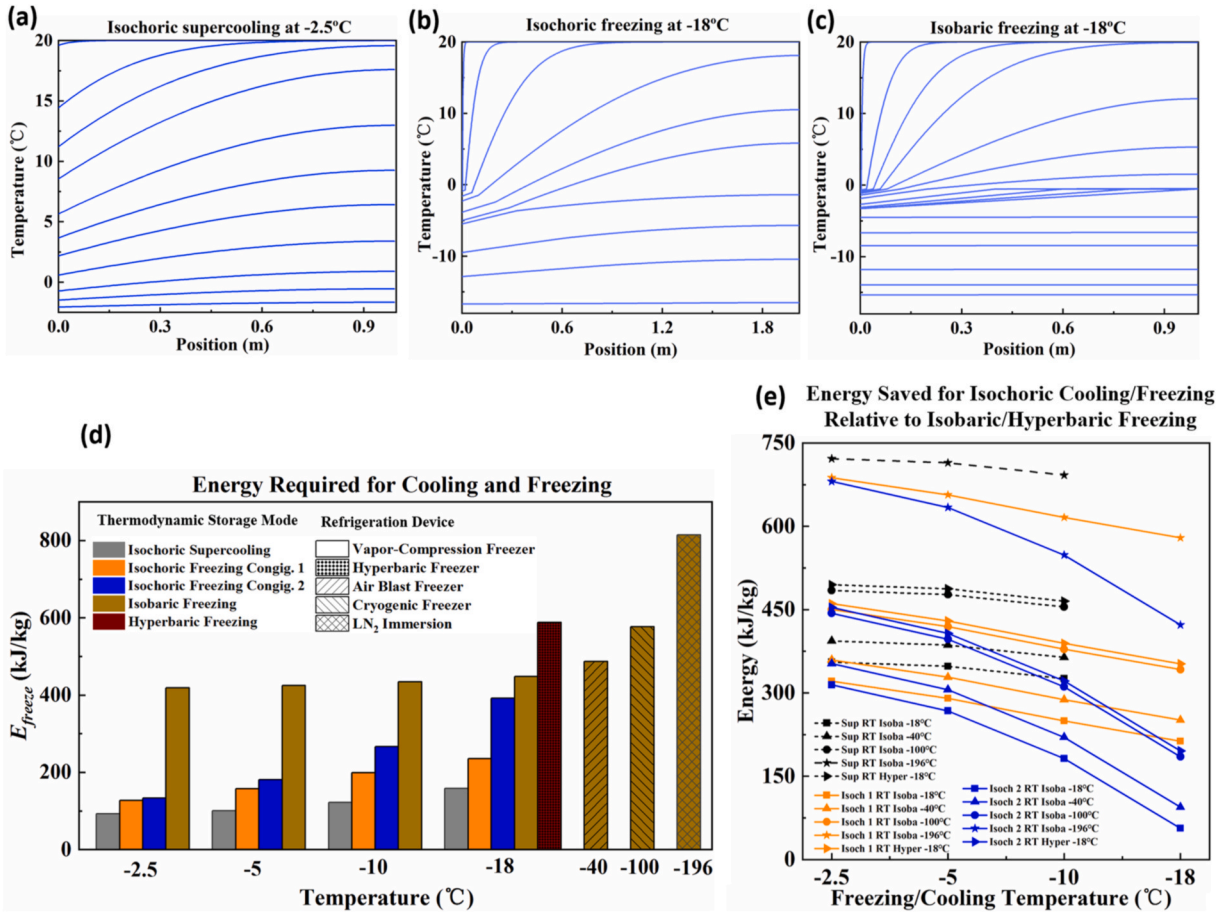

Fig. 3. Temperature and energy during initial cooling/freezing. **(a–c) Temperature profiles during freezing for different methods.** (**a**) Temperature profiles during isochoric supercooling at −2.5 °C. (**b**) Temperature profiles during isochoric freezing (configuration 2) at −18 °C. (**c**) Temperature profiles during isobaric freezing at −18 °C. (**d-e**) **Energy consumption of different freezing modes per kg food. (d)** Energy consumption during the freezing process for different thermodynamic systems. **(e)** Energy saved during cooling/freezing by isochoric supercooling (at −2.5, −5 and −10 °C), isochoric config. 1 (at −2.5, −5, −10, −18 °C), isochoric config. 2 (at −2.5, −5, −10, −18 °C) relative to conventional freezing (hyperbaric at −18° and isobaric at −18, −40, −100, −196 °C).

2.2.2. Energy required for isobaric freezing

For the simple case of freezing under isobaric conditions at constant atmospheric pressure (the current industry standard), the energy required during freezing can be totaled as:

$$E_{freeze} = m\cdot\left[\int_{T_0}^{T_f} c_{p,liquid}(T)dT + \int_{T_f}^{T_{storage}} c_{p,ice}(T)dT + H\right] \tag{16}$$

in which $c_p(T)$ is the temperature-dependent isobaric specific heat capacity and H is the specific latent heat of fusion of ice.

2.2.3. Energy required for isochoric freezing

The isochoric case differs in two key aspects: firstly, only a portion of the system will freeze, with the equilibrium state presenting a two-phase pressurized liquid-ice equilibrium per Fig. 2; secondly, due to the aforementioned pressurization (which occurs as a result of ice expanding under physical confinement and is a direct function of temperature), the freezing point of the system will continuously decrease as freezing progresses. These aspects require alteration of Eqn. (16) to include the term $\phi(T)$ describing the fraction of the system mass which will freeze at a given sub-zero temperature, which has been calculated according to our previous work [19], and to include a temperature-dependent latent heat of fusion $H(T)$. Armed with these terms, the energy required to freeze the modified mass of food under isochoric conditions is:

$$E_{freeze} = m_{isochoric}\left[\int_{T_0}^{T_{storage}} (1-\phi(T))c_{v,liquid}(T)dT + \int_{T_f}^{T_{storage}} \phi(T)\cdot c_{v,ice}(T)dT + \int_{T_f}^{T_{storage}} \phi(T)\cdot H(T)dT\right] \tag{17}$$

Here $c_v(T)$ is the specific heat capacity at constant volume. Numerical values for all parameters are available in the SI.

2.2.4. Energy required for isochoric supercooling

In addition to the isochoric and isobaric freezing processes described in Eqn. (16) and (17) of the main text, we examined two other thermodynamic modes for initial cooling/freezing: isochoric supercooling and hyperbaric freezing.

Isochoric supercooling is a process by which the system is chilled only mildly below its freezing temperature and held in a metastable supercooled liquid state [24]. The application of supercooling within food preservation has been investigated for several years, but has gained little traction to the instability of supercooled systems under isobaric conditions, in which small perturbations can cause the system to destabilize and freeze entirely. Isochoric conditions have recently been found to significantly stabilize supercooled conditions, potentially pacing the way to more widespread use in industrial environments. However, it should be noted that the thermodynamic description of isochoric supercooling provided below will be nearly identical in the case of

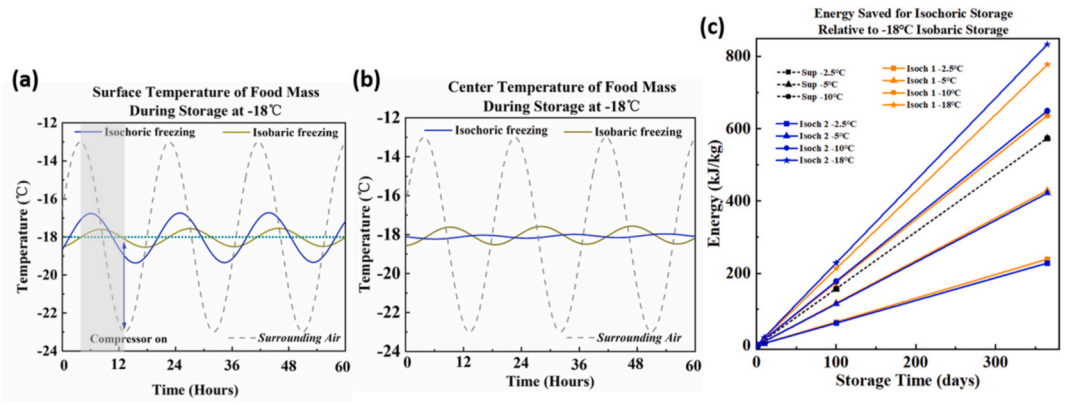

Fig. 4. Temperature and energy during cold storage. (**a**) Temperature response at the surface of the food mass for isochoric (config. 2) and isobaric systems. (**b**) Temperature response in the center of the food mass for isochoric (config. 2) and isobaric systems. (**c**) Energy saved during storage for per kg food for 365 days by isochoric supercooling (at −2.5, −5 and −10 °C), isochoric config. 1 (at −2.5, −5, −10, −18 °C), isochoric config. 2 (at −2.5, −5, −10, −18 °C) relative to the energy for storage in isobaric system at −18 °C.

isobaric supercooling, differing only in the use of the isochoric vs. isobaric heat capacities.

2.3. The energy required for isochoric supercooling per kilogram food is

$$E_{freeze} = \left[\int_{T_0}^{T_{storage}} c_{v,water}(T)dT \right] \tag{18}$$

For isochoric freezing, isobaric freezing and isochoric supercooling processes, the electrical work consumed by the compressor to provide energy for per kilogram food can be calculated using the appropriate COP from Table 1b of the main text as:

$$W = \frac{E_{freeze}}{COP} \frac{1}{3.6 \times 10^6} \tag{19}$$

2.3.1. Energy required for hyperbaric freezing

For hyperbaric freezing, a rigid container is loaded with food products immersed in pure water. The food-water system in the container is pressurized by a compressor prior to cooling. This depresses the freezing point of the system, allowing it to cool to significantly lower temperatures before the onset of freezing. Once the system has been chilled in the pressurized liquid phase to some designated sub-zero centigrade temperature, the pressure is mechanically released, causing rapid low-temperature ice formation that results in much smaller characteristic ice crystal sizes, in turn reducing damage to the cellular integrity of the stored foods.

To calculate the minimum energy required for the hyperbaric freezing process, three energy-consuming steps are considered [13]:

(1) Compression of the food at 20 °C from 0.1 MPa to 180 MPa:

$$E_{compression} = \int_{P_0}^{P} VdP = \int_{P_0}^{P} L{\cdot}AdP \Big/ m$$

(2) Cooling of the unfrozen food at 180 MPa to the desired storage temperature (herein −18 °C):

$$E_{cooling-hyperbaric} = m{\cdot} \int_{T_0}^{T_1} c_{p,water}(T)dT$$

Note that the food will not freeze en route to −18 °C if pressurized to 180 MPa.

(3) Isentropic expansion to atmospheric pressure and freezing of food at −18 °C:

The minimum total energy required for hyperbaric freezing per kilogram food (as plotted in Fig. 3a) is thus given by

$$E_{freeze} = \left[\int_{P_0}^{P} VdP + \int_{T_0}^{T_{storage}} c_{p,water}(T)dT + H(T_{storage}) \right] \tag{20}$$

Note herein that the pressure-dependence of the specific heat capacity has been neglected for simplicity.

The electrical work consumed by the hyperbaric freezer contains freezing and compressing process, which is

$$W = \left(\frac{E_{freeze} - E_{compression}}{COP} + \frac{E_{compression}}{\eta} \right) \cdot \frac{1}{3.6 \times 10^6} \tag{21}$$

where the efficiency of the compressor is assumed as $\eta = 0.6$ [43].

2.4. Extended storage

Having dealt with the freezing process itself, the second part of our model estimates the energy required to store the food mass in its frozen state continuously. To this end, we assume storage in a simple domestic vapor-compression freezer with a known temperature-dependent coefficient of performance (Table 1b). In order to reduce compressor running time, such devices typically operate on an on/off compression cycle, which yields continuous temperature fluctuation within the device. We will herein model this fluctuation as a sin wave $B\,sin(\omega t)$ centered on the desired storage $T_{storage}$, with a constant amplitude B and frequency ω. Assuming this oscillating temperature within the air of the refrigerator cabinet, we adapt the discrete 1D thermal phase change model (the domain for which is shown schematically in Fig. 2d) to calculate the energy exchange between the refrigerated air and the stored food mass. For simplicity, we assume that the refrigerated air surrounding the food mass is much greater in volume than the food itself, and that the temperature profile of the air may be prescribed by the steady-periodic form

$$T_{air} = T_{storage} + B{\cdot}\sin(wt) \tag{22}$$

in which the amplitude and frequency were chosen based on [40].

2.5. Initial conditions

For the cold storage period, the temperature of the food system in all thermodynamic cases is initialized as spatially uniform at the desired storage temperature.

$$T(x,\ t=0) = T_{storage} \tag{23}$$

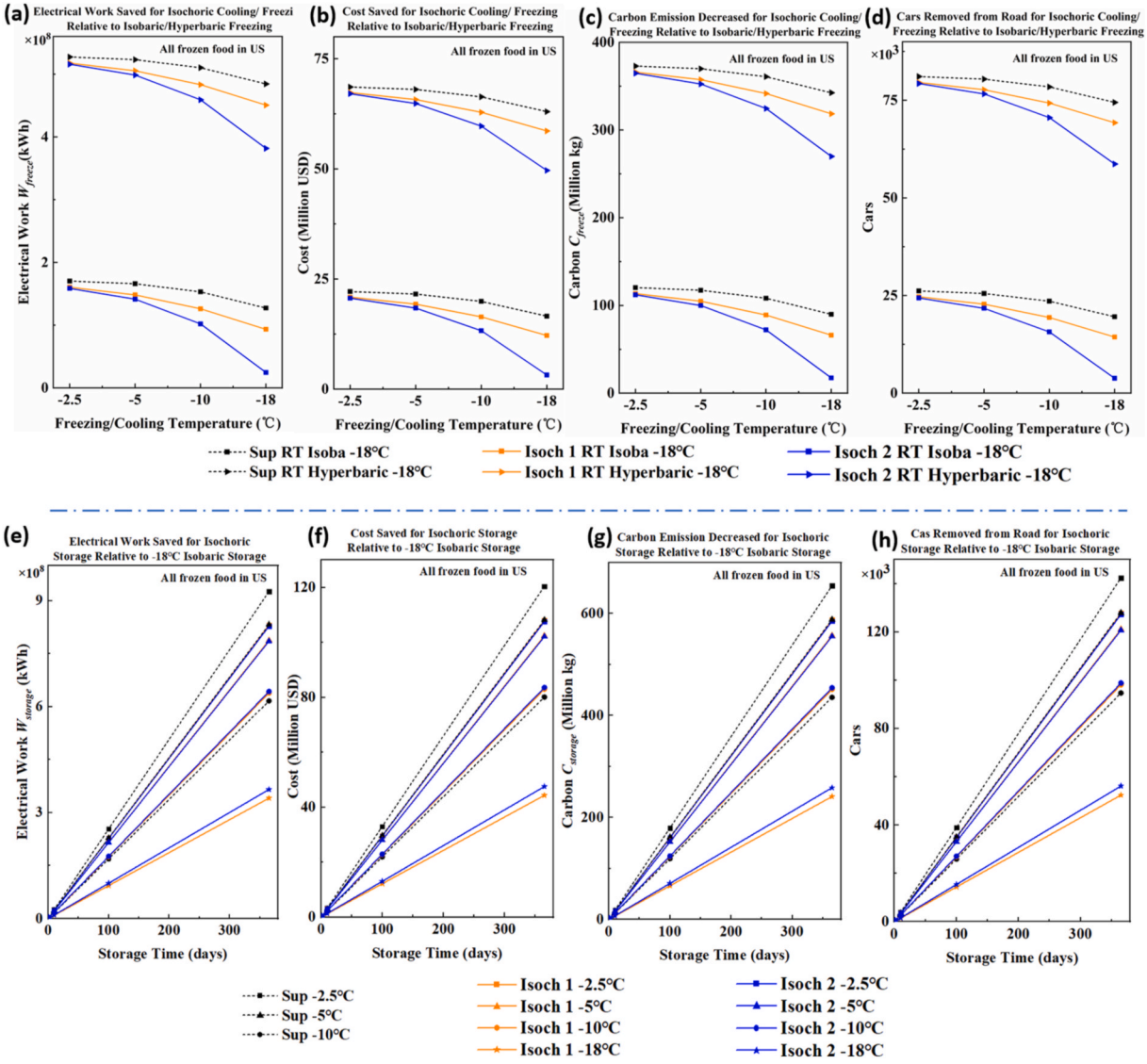

Fig. 5. Comparison of energy savings from isochoric freezing and storage for all frozen food in the U.S. (**a**) Electrical work saved, (**b**) Cost saved, (**c**) Carbon Emission Decreased, (**d**) Cars removed from road during cooling and freezing by isochoric supercooling (at −2.5, −5 and −10 °C), isochoric config. 1 (at −2.5, −5, −10, −18 °C), isochoric config. 2 (at −2.5, −5, −10, −18 °C) relative to conventional freezing (hyperbaric at −18 °C and isobaric at −18, −40, −100, −196 °C). (**e**) Electrical work saved, (**f**) Cost saved, (**g**) Carbon emission decreased, (**h**) Cars removed from road during storage for 365 days by isochoric supercooling (at −2.5, −5 and −10 °C), isochoric config. 1 (at −2.5, −5, −10, −18 °C), isochoric config. 2 (at −2.5, −5, −10, −18 °C) relative to the energy for storage in isobaric system at −18 °C.

2.6. Boundary conditions

Convective exchange at the exterior surface of the system:

$$h\left(T_{air} - T_{surface}\right) = k_s \frac{\partial T}{\partial x}\Big|_{x=0} \; at \; x = 0, \; t > 0 \tag{24}$$

in which h is the natural convective heat transfer coefficients between the refrigerated air and the stored food mass.

Insulated symmetry boundary at the center of the system:

$$\frac{\partial T}{\partial x}\Big|_{x=L} = 0 \; at \; x = L, \; t > 0 \tag{25}$$

To calculate the temperature profile and interface position as a function of time, Eqns. (1)–(9), Eqns. 12 and 13 and Eqns. 22–25 are solved using MATLAB software. Following the method used in Ref. [40], which represents a front-tracking method similar to that employed in Ref. [44] but modified for isochoric conditions, in order to solve the isochoric freezing and storage equations the energy balance equation on the solid-liquid interface Eqn. (3) is treated as an independent equation whose solution gives the quasi-steady position of the interface in time.

Firstly, time is discretized in all of the resulting equations as

$$t = j \cdot \Delta t, \; \Delta t = cons \tan t, \; j \in N \tag{26}$$

Herein, j represents the timestep number. In the following, the subscript j represents the value of a given parameter at step j in time.

The movement of the phase change interface drives the iterative solution scheme. For a timestep Δt, the distance Δx that the interface moves from its previous position is calculated using the interfacial energy balance Eqn. (3). The phase change interface position is updated as

$$\delta_j = \delta_{j-1} + \Delta x \tag{27}$$

As freezing progresses, the mass percent of the ice in the system can be calculated from the phase change interface position using

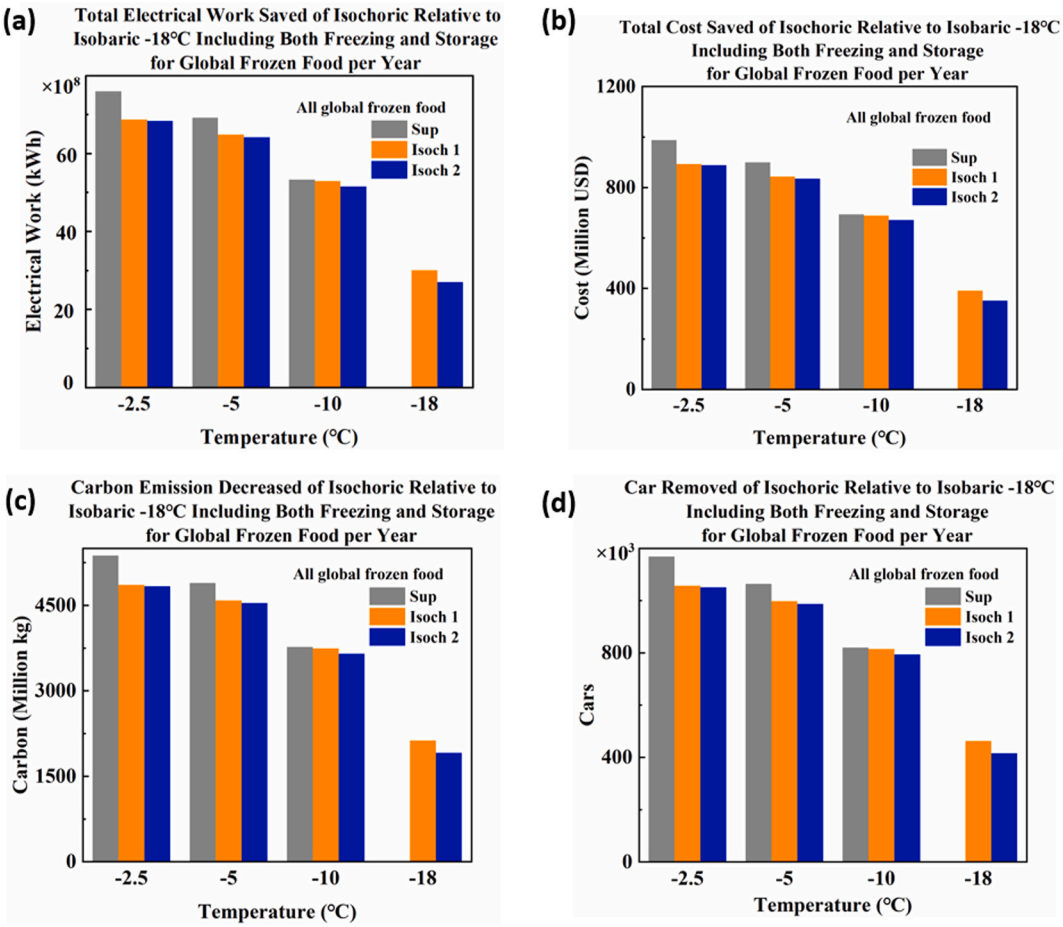

Fig. 6. Comparison of energy savings from isochoric freezing and storage for the global frozen food. (**a**) Total energy saved, (**b**) Cost saved, (**c**) Carbon emission decreased, (**d**) Equivalent to total cars removed from road relative to conventional isobaric freezing and storage for one year at −18 °C.

$$\phi_j = \frac{\delta_j}{L}\frac{\rho_s}{\rho_l}\cdot 100 \tag{28}$$

For each iteration, the pressure in the system $P(\phi)$ can be calculated according to Eqn. (7), and the new phase change temperature of the system $T_f(P)$ corresponding to the updated hydrostatic pressure can be calculated in turn according to Eqn. (6). Once the phase change temperature and Δx have been obtained, they are used to re-solve the governing equations given in Eqns. (1)–(9) for the temperature profiles within the frozen and unfrozen regions, which are then used to re-solve the interfacial balance equation Eqn. (3) and generate a new value of Δx. This process proceeds iteratively for a given timestep j until the distance Δx the interface has moved converges to within a predetermined convergence criterion (10^{-9}).

For the cold storage (isochoric supercooled, isochoric frozen and isobaric frozen) stage for 365 days, the energy required for storage per kilogram food by the compressor of the freezer is calculated by totaling the convective exchange between the cooled air and the food product during the time-portion of the temperature cycle in which the compressor is running, as indicated by the air temperature decreasing. This exchange is written as:

$$E_{storage} = A\cdot \int_0^{t_{compressor}} \left|h\left(T_{air} - T_{surface}\right)\right| dt,\ x = 0 \tag{29}$$

To reiterate, $t_{compressor}$ is the time period in which the compressor is running, e.g. the time period over which the prescribed oscillating air temperature is *decreasing*.

The electrical work consumed by the compressor to provide this energy for 365 days per kilogram food can then be calculated using the appropriate COP from Table 1b of the main text as:

$$W = \frac{E_{storage}}{COP}\cdot\frac{1}{3.6\times 10^6} \tag{30}$$

2.7. Energy savings calculations

Here we analyze the energy savings, electrical cost savings, carbon emission savings for food storage at subfreezing temperature under isochoric conditions relative to isobaric conditions. The electrical work W_{freeze} consumed by freezer for freezing and storage in the U.S. or the world are given by

$$W_{freeze} = \frac{E_{freeze}}{COP}\cdot\frac{1}{3600}\cdot M \tag{31}$$

$$W_{storage} = \frac{E_{storage}}{COP}\cdot\frac{1}{3600}\cdot M \tag{32}$$

where M is the total frozen food in mass. Employing an average electricity cost of $0.13 per kWh. The electricity cost for freezing and storage is

$$COST_{freeze} = \frac{E_{freeze}}{COP}\cdot\frac{1}{3600}\cdot M\cdot 0.13 \tag{33}$$

$$COST_{storage} = \frac{E_{storage}}{COP}\cdot\frac{1}{3600}\cdot M\cdot 0.13 \tag{34}$$

The carbon emission equivalency factor recommended by the U.S.

Environmental Protection Agency (0.707 $\frac{kg\ CO_2}{kWh}$) [45]. The carbon emission is for freezing and storage is

$$C_{freeze} = \frac{E_{freeze}}{COP} \cdot \frac{1}{3600} \cdot M \cdot 0.707 \quad (35)$$

$$C_{storage} = \frac{E_{storage}}{COP} \cdot \frac{1}{3600} \cdot M \cdot 0.707 \quad (36)$$

3. Results and discussion

3.1. Energy savings during the initial freezing stage

The temperature profile of the system at progressing timepoints under different freezing methods is shown in Fig. 3a-c. Fig. 3a depicts isochoric supercooling, which is a single-phase process and thus has no phase-change interface. Fig. 3b depicts isochoric freezing, in which the phase-change interface can be seen to decrease in temperature as it progresses, due to the pressurization that ice growth causes within the system and the according depression of the freezing point. Note further that the phase-change interface stops short of the end of the domain, consistent with the limited ice formation seen in isochoric systems. Fig. 3c depicts isobaric freezing, in which the phase-change interface progresses across the entire domain and the temperature at the interface (the freezing point of the system) remains approximately constant. In reality during both isochoric and isobaric freezing there will be mild additional freezing point depression driven solute rejection from the ice phase, but given the extremely dilute starting concentration, these effects were neglected.

The findings of our model in regards to energy savings during the initial freezing stage are presented in Fig. 3d and e. The plots in Fig. 3d show the energy consumed during freezing per kg of food, with various methods. Fig. 3e shows the energy savings (e.g. the difference in energy consumed) per mass of preserved food between isochoric systems and various isobaric methods as a function of isochoric storage temperature. The results demonstrate that both isochoric freezing and isochoric supercooling can significantly reduce the energy expenditure required for food for cold storage at a range of subfreezing temperatures.

The principal mechanism driving these savings is the avoidance of total conversion of the isochoric system to ice. This provides a dramatic reduction in the energy required to bring the mass to steady-state at subfreezing temperatures, driven by a large reduction in latent heat consumption (and noting that the specific latent heat of ice is roughly two orders of magnitude larger than the sensible specific heat capacity of water). For isochoric freezing, the relative reduction in energy is a product both of reduced latent heat consumption and also the fact that the specific latent heat associated with formation of ice decreases at lower temperatures [46]. The temperature-dependence of the isochoric ice percentage (Figs. 2b and 3b) also drives the increasing differences observed between the two possible isochoric freezing configurations. In the case of isochoric supercooling the energy savings results are more straight-forward, as the system remains in an entirely unfrozen, metastable state (Fig. 3a); the difference between the supercooled and isobaric energy consumption is simply equal to the latent heat of fusion and the minor differences between the heat capacities of liquid water and ice.

The results of Fig. 3d demonstrate that isochoric conditions, be they metastable (isochoric supercooling) or equilibrium (isochoric freezing) invariably reduce the energy consumed during the initial chilling/freezing process. Furthermore, Fig. 3e shows that extreme savings in latent heat expenditure may be attainable by storing foods at higher subzero temperatures under isochoric conditions. As mentioned earlier, isochoric cold storage is not affected by ice recrystallization. These temperature-sensitive energy savings prove unattainable by comparison in conventional isobaric systems, because water will convert entirely to ice at all temperatures below the freezing point when exposed to a constant pressure reservoir such as the atmosphere.

As mentioned earlier tomatoes [27], spinach [28], cut potatoes [29], sweet cherries [30], tilapia [47] stored in an isochoric system at temperatures between −2.5 °C and −7 °C, are of substantial higher quality than similar foods preserved by conventional isobaric freezing methods. The absence of ice crystals in isochoric freezing and cold storage eliminates the need for low temperature freezing to produce small ice crystals and the use of low temperature storage to avoid recrystallization – al this while the quality of the food product is improved.

In addition to improved food quality, storing food in optimal isochoric conditions also saves energy. As an example, per Fig. 3e, use of isochoric supercooling at −2.5 °C can save 355.44 kJ per kg food compared to conventional isobaric freezing at −18 °C, and isochoric freezing (configuration 1) at −5 °C can save 290.26 kJ per kg of food compared to the same.

3.2. Energy savings during prolonged cold storage

Fig. 4a and b compare the temperature fluctuations on the outer surface and the center of a comparable slab like geometry during isochoric and isobaric storage at −18 °C. These figures illustrate another advantage of isochoric cold storage relative to isobaric cold storage. Temperature fluctuation during storage and distribution of frozen foods can result in cycles of thawing and refreezing and recrystallization of ice crystals and in drip loss, e.g. Ref. [48], which are detrimental to the quality of the frozen food. This mode of damage does not exist in isochoric storage. Furthermore, it is important to note that the change of phase interface in the isochoric system acts as a temperature-stabilizing PCM (phase change material), a well-known mechanism for energy savings and storage [49,50]. This leads to the findings that sustained storage of foods frozen under isochoric conditions requires less electrical work from the refrigerating device than conventional isobaric storage. Energy savings attributable to prolonged isochoric cold storage as compared to isobaric cold storage as a function of storage time are shown in Fig. 4c. Isochoric ice-free storage (config. 1) at −5 °C will save 429.21 kJ energy per kg food annually relative to conventional isobaric storage at −18 °C. As mentioned in the previous paragraph, there is no ice recrystallization in isochoric cold storage and therefore the storage temperature is not constrained by the need to eliminate ice recrystallization.

3.3. US and global energy savings from transition to isochoric cold storage

The work presented herein suggests that isochoric conditions may present a unique cold food storage alternative with the potential to both enhance food quality and significantly reduce energy consumption. Furthermore, this storage approach does not require substantial modification of the current global refrigeration infrastructure, as isochoric thermodynamics are enforced at the storage-container scale; thus, isochoric storage capabilities (for freezing or supercooling alike) could theoretically be built into any existing cold-storage facility.

Fig. 5 gives the potential savings in the US made possible by transition from isobaric to isochoric freezing and storage, separated by savings during the initial cooling/freezing process and savings during prolonged storage. The 2019 cold storage frozen food volume in the U.S. was 4.52 billion kg [51]. Fig. 5a–d demonstrate various savings associated with the use of isochoric processes as compared to conventional isobaric or hyperbaric freezing to −40 °C. Depicted respectively are the annual electrical work saved, the associated energy cost saved, the carbon emissions averted, and the number of cars removed from the road required to produce equivalent carbon savings. Fig. 5a–d, show that for freezing to any cold storage temperature, isochoric freezing consumes less energy than isobaric freezing. As discussed in previous sections, isochoric storage does not require the low storage temperatures required by isobaric freezing. The experiments listed earlier show that −5 °C may be an optimal temperature for isochoric cold storage. As an

example of energy savings, isochoric cold storage in configuration 1 at −5 °C saves in the US annually, relative to isobaric freezing to −18 °C, 148 million kWh of electricity, at a cost of 19.28 million USD, and reduces emissions of CO_2 by 104.87 million kg, equivalent to the removal of roughly 23,000 cars from the road. Figures, 5e-h provide the same savings metrics for prolonged isochoric storage at various subfreezing temperatures as compared to isobaric cold storage at - 18 °C. For example, isochoric storage in configuration 2 at −5 °C saves 790 million kWh (equivalent to 102.13 million USD) and 560 million kg of CO_2 annually.

Finally, Fig. 6 shows potential savings due to a transition from isobaric freezing and storage at −18 °C to isochoric freezing and storage at various temperatures for the global frozen food market. The total global frozen food capacity in 2019 was approximately 31.3 billion kg [52]. If all of this food was processed under isochoric conditions (config. 1) at −5 °C rather than under isobaric conditions at the industry-standard of −18 °C, a total savings of 6.49 billion kWh could be realized. This energy saving translates to an annual economic savings of approximately 843.33 million USD and an annual environmental savings of 4.59 billion kg of CO_2 (equivalent to removing of roughly one million cars from the road [45]).

4. Conclusions

In summary, we developed a simple two-part phase change model to describe the thermodynamics of frozen food storage in several thermodynamic storage modes: traditional isobaric freezing; hyperbaric (or pressure-shift) freezing; isochoric freezing, and isochoric supercooling, which we evaluate at several storage temperatures reflecting various processes found in industry. The model treats separately the two thermodynamically significant steps of the food cold-storage process: initial cooling and freezing and extended storage. The energy savings, reduction in global energy burden, and reduction in carbon footprint that could be accrued from transitioning the global food cold chain from isobaric cold storage to isochoric cold storage are analyzed. The result shows that the energetic costs of frozen food storage could be dramatically reduced by isochoric cold storage without significant changes to global refrigeration infrastructure and whilst increasing frozen food quality. Furthermore, the ability to preserve freeze sensitive foods could reduce food waste and open new global markets. Isochoric cold storage technology results in substantially improved quality of the preserved food, greatly extended periods of preservation, and long-term preservation of foods that cannot be preserved by other freezing methods, and it has the potential for significant cross-cutting impacts in medical and scientific biopreservation. While this study is theoretical in nature and broad in scope, our results suggest that isochoric cold storage may prove a compelling alternative to conventional freezing techniques for the cold storage of food and beyond.

Data availability

All data available upon request.

Author contributions

YHZ, BR and MPP conceived the work. YHZ and JJW performed the calculations. MPP and BR wrote the manuscript, with assistance from YHZ. CB and TM provided the experimental data on food storage quality. MPP edited the manuscript.

Declaration of competing interest

The authors declare the following financial interests/personal relationships which may be considered as potential competing interests: The authors Boris Rubinsky and Matt Powell-Palm are leading an early stage start up in the field of isochoric preservation named “BioChoric”, which could be perceived as potential competing interests.

The other authors have no known competing financial interests.

Acknowledgments

This work is supported by the USDA National Institute of Food and Agriculture, AFRI project Proposal #: 2017–05031, Award # 2018-67017-27826 “Preservation of food by isochoric (constant volume) freezing” and by the NSF Engineering Research Center for Advanced Technologies for Preservation of Biological Systems (ATP-Bio) NSF EEC #1941543. YHZ was supported by the Scholarship of China Scholarship Council. Special thanks to Dr. Jue Wang from University of Chinese Academy of Sciences for helpful assistance with the MATLAB programming.

Appendix A. Supplementary data

Supplementary data to this article can be found online at https://doi.org/10.1016/j.rser.2021.111621.

References

[1] Gustavsson J, Cederberg C, Sonesson U, van Otterdijk R, Meybeck A. Global food losses and food waste: extent, causes and prevention. https://reliefweb.int/report/world/global-food-losses-and-food-waste-extent-causes-and-prevention. [Accessed 9 March 2021].
[2] Bond M, Meacham T, Bhunnoo R, Benton TG. Food waste within global food systems, glob food secur program. http://cradall.org/sites/default/files/food-waste-report_0.pdf. [Accessed 9 March 2021].
[3] Dupont JL, El Ahmar A, Guilpart J. The role of refrigeration in worldwide nutrition. In: 6th informatory note on refrigeration and food; 2020. 2020, https://iifiir.org/en/fridoc/the-role-of-refrigeration-in-worldwide-nutrition-2020-142029. [Accessed 8 March 2021].
[4] Archer DL. Freezing: an underutilized food safety technology? Int J Food Microbiol 2004;90:127–38. https://doi.org/10.1016/S0168-1605(03)00215-0.
[5] Research and Markets. Frozen food market by product type and user: global opportunity analysis and industry forecast, 2020-2027. https://www.businesswire.com/news/home/20200 825005521/en/Global-Frozen-Food-Market-2020-to-2027—by-Product-Type-and-User—ResearchAndMarkets.com. [Accessed 16 February 2021].
[6] Dupont JL, Domanski P, Lebrun P, Ziegler F. The role of refrigeration in the global economy (2019), 38th note on refrigeration technologies. https://iifiir.org/en/fridoc/142028. [Accessed 9 March 2021].
[7] United States Environmental Protection Agency. Greenhouse gases equivalencies calculator - calculations and references. https://www.epa.gov/energy/greenhouse-gases-equivalencies-calculator-calculations-and-refere nces#:~:text=The%20national%20weighted%20average%20carbon,and%20distribution%20(EPA%202019). [Accessed 9 March 2021].
[8] Tan M, Mei J, Xie J. The Formation and control of ice crystal and its impact on the quality of frozen aquatic products: a review. Crystals 2021;11:68. https://doi.org/10.3390/cryst11010068.
[9] Li D, Zhu Z, Sun D-W. Effects of freezing on cell structure of fresh cellular food materials: a review. Trends Food Sci Technol 2018;75:46–55. https://doi.org/10.1016/j.tifs.2018.02.019.
[10] Foster ED. Ouick-freezing and the perishable food problem. Harv Bus Rev 1934.
[11] Arthey D. Managing frozen foods. Trends Food Sci Technol 2001;12:42–3. https://doi.org/10.1016/S0924-2244(01)00047-4.
[12] Sun DW. Handbook of frozen food processing and packaging. https://doi.org/10.1016/j.tifs.2012.07.001; 2005.
[13] Kalichevsky MT, Knorr D, Lillford PJ. Potential food applications of high-pressure effects on ice-water transitions. Trends Food Sci Technol 1995;6:253–9. https://doi.org/10.1016/S0924-2244(00)89109-8.
[14] Zhu Z, Li T, Sun DW. Pressure-related cooling and freezing techniques for the food industry: fundamentals and applications. Crit Rev Food Sci Nutr 2020:1–16. https://doi.org/10.1080/10408398.2020.1841729.
[15] Hartel RW. Advances in food crystallization. Annu Rev Food Sci Technol 2013;4:277–92. https://doi.org/10.1146/annurev-food-030212-182530.
[16] Mahlia TMI, Saidur R. A review on test procedure, energy efficiency standards and energy labels for room air conditioners and refrigerator-freezers. Renew Sustain Energy Rev 2010;14:1888–900. https://doi.org/10.1016/j.rser.2010.03.037.
[17] McLinden MO, Seeton CJ, Pearson A. New refrigerants and system configurations for vapor-compression refrigeration. Science 2020;370:791–6. https://doi.org/10.1126/science.abe3692.
[18] Kasaeian A, Hosseini SM, Sheikhpour M, Mahian O, Yan WM, Wongwises S. Applications of eco-friendly refrigerants and nanorefrigerants: a review. Renew Sustain Energy Rev 2018;96:91–9. https://doi.org/10.1016/j.rser.2018.07.033.
[19] Rubinsky B, Perez PA, Carlson ME. The thermodynamic principles of isochoric cryopreservation. Cryobiology 2005;50:121–38. https://doi.org/10.1016/j.cryobiol.2004.12.002.

[20] Szobota SA, Rubinsky B. Analysis of isochoric subcooling. Cryobiology 2006;53:139–42. https://doi.org/10.1016/j.cryobiol.2006.04.001.
[21] Preciado JA, Rubinsky B. Isochoric preservation: a novel characterization method. Cryobiology 2010;60:23–9. https://doi.org/10.1016/j.cryobiol.2009.06.010.
[22] Powell-Palm MJ, Rubinsky B, Sun W. Freezing water at constant volume and under confinement. Commun Phys 2020;3:1–8. https://doi.org/10.1038/s42005-020-0303-9.
[23] Powell-Palm MJ, Aruda J, Rubinsky B. Thermodynamic Theory and experimental validation of a multiphase isochoric freezing process. J Biomech Eng 2019;141:1–8. https://doi.org/10.1115/1.4043521.
[24] Powell-Palm MJ, Koh-Bell A, Rubinsky B. Isochoric conditions enhance stability of metastable supercooled water. Appl Phys Lett 2020:123702. https://doi.org/10.1063/1.5145334.
[25] Nastase G, Lyu C, Ukpai G, Serban A, Rubinsky B. Isochoric and isobaric freezing of fish muscle. Biochem Biophys Res Commun 2017;485:279–83. https://doi.org/10.1016/j.bbrc.2017.02.091.
[26] Lyu C, Nastase G, Ukpai G, Serban A, Rubinsky B. A comparison of freezing-damage during isochoric and isobaric freezing of the potato. PeerJ 2017;2017:1–15. https://doi.org/10.7717/peerj.3322.
[27] Bilbao-Sainza C, Sinrod AJG, Dao L, Takeoka G, Williams T, Wood D, et al. Preservation of grape tomato by isochoric freezing. Food Sci Int 2021;143:110228. https://doi.org/10.1016/j.foodres.2021.110228.
[28] Bilbao-Sainz C, Sinrod AGJ, Dao L, Takeoka G, Williams T, Wood D, et al. Preservation of spinach by isochoric (constant volume) freezing. Int J Food Sci Technol 2020;55:2141–51. https://doi.org/10.1111/ijfs.14463.
[29] Bilbao-Sainz C, Zhao Y, Takeoka G, Williams T, Wood D, Chiou B, et al. Effect of isochoric freezing on quality aspects of minimally processed potatoes. J Food Sci 2020;85:2656–64. https://doi.org/10.1111/1750 -3841.15377.
[30] Bilbao-Sainz C, Sinrod A, Powell-Palm MJ, Dao L, Takeoka G, Williams T, et al. Preservation of sweet cherry by isochoric (constant volume) freezing. Innovat Food Sci Emerg Technol 2019;52:108–15. https://doi.org/10.1016/j.ifset.2018.10.016.
[31] MCHugh T, Bilbao-Sainz C, Rubinsky B, Powell-Palm MJ. Isochoric impregnation of solid foods at subfreezing temperatures. U.S. Provisional patent 63,159,528.
[32] Bridges DF, Bilbao-Sainz C, Powell-Palm MJ, Williams T, Wood D, Sinrod AJG, et al. Viability of listeria monocytogenes and salmonella typhimurium after isochoric freezing. J Food Saf 2020;40:e12840. https://doi.org/10.1111/jfs.12840.
[33] Powell-Palm MJ, Preciado J, Lyu C, Rubinsky B. Escherichia coli viability in an isochoric system at subfreezing temperatures. Cryobiology 2018;85:17–24. https://doi.org/10.1016/j.cryobiol. 2018.10.262.
[34] Giwa S, Lewis JK, Alvarez L, Langer R, Roth AE, Church GM, et al. The promise of organ and tissue preservation to transform medicine. Nat Biotechnol 2017;35(6):530–42. https://doi.org/10.1038/nbt.3889.
[35] Buriak I, Fleck RA, Goltsev A, Shevchenko N, Petrushko M, Yurchuk T, et al. Translation of cryobiological techniques to socially economically deprived populations—Part 1: cryogenic preservation strategies. J Med Devices 2020;14. https://doi.org/10.1115/1.4045878.
[36] Wan L, Powell-Palm MJ, Lee C, Gupta A, Weegman B, Clemens MG, et al. Preservation of rat hearts in subfreezing temperature isochoric conditions to -8° C and 78 MPa. Biochem Bioph Res Co 2018;496(3):852–7. https://doi.org/10.1016/j.bbrc.2018.01.140.
[37] Powell-Palm MJ, Charwat V, Charrez B, Siemons BA, Healy KE, Rubinsky B. Isochoric supercooled preservation and revival of human cardiac microtissues. bioRxiv 2021. https://doi.org/10.1101/2021.03.22. 436466.
[38] Powell-Palm MJ, Zhang Y, Aruda J, Rubinsky B. Isochoric conditions enable high subfreezing temperature pancreatic islet preservation without osmotic cryoprotective agents. Cryobiology 2019;86:130–3. https://doi.org/10.1016/j.cryobiol.2019.01.003.
[39] Nastase G, Perez PA, Serban A, Dobrovicescu A, Stefanescu MF, Rubinsky B. Advantages of isochoric freezing for food preservation: a preliminary analysis. Int Commun Heat Mass Tran 2016;78:95–100. https://doi.org/10.1016/j.icheatmasstransfer.2016.08.026.
[40] Powell-Palm MJ, Rubinsky B. A shift from the isobaric to the isochoric thermodynamic state can reduce energy consumption and augment temperature stability in frozen food storage. J Food Eng 2019;251:1–10. https://doi.org/10.1016/j.jfoodeng.2019.02.001.
[41] Perez PA. Thermodynamic and heat transfer analysis for isochoric cryopreservation. PhD Thesis. Berkeley CA: University of California at Berkeley; 2006.
[42] Zhao Y, Powell-Palm MJ, Ukpai G, Bilbao-Sainz C, Chen L, Wang J, et al. Phase change interface stability during isochoric solidification of an aqueous solution. Appl Phys Lett 2020;117. https://doi.org/10.1063/5. 0019878.
[43] Ramsey M. Practical wellbore hydraulics and hole cleaning 2019. first ed. Gulf Professional Publishing; 2019.
[44] Yoo J, Rubinsky B. Numerical computation using finite elements for the moving interface in heat transfer problems with phase transformation. Numer Heat Tran 1983;6:209–22. https://doi.org/10.1080/01495728308963083.
[45] United States Environmental Protection Agency. Greenhouse gas emissions from a typical passenger vehicle. . [Accessed 6 February 2021]. nepis.epa.gov/Exe/ZyNET.exe/P100LQ99.TXT?ZyActionD=ZyDocument&Client=EPA& Index=2011+Thru+2015&Docs=&Query=&Time=&EndTime=&SearchMethod=1&TocRestrict=n&Toc=&TocEntry=&QField=&QFieldYear=&QFieldMonth=&QFieldDay=&IntQFieldOp=0&ExtQFieldOp=0&XmlQuery=&File=D%3A%5Czyfiles%5CIndex%20Data%5C11thru15%5CTxt%5C00000014%5CP100LQ99.txt&User=ANONYMOUS&Password=anonymous&SortMethod=h%7C-&MaximumDocuments =1&Fuzzy Degree=0&ImageQuality=r75g8/r75g8/x150y150g16/i425&Display=hpfr&DefSeekPage=x&SearchBack=ZyActionL&Back=ZyActionS&BackDesc=Results%20page&MaximumPages=1&ZyEntry=1&SeekPage=x&ZyPURL;.
[46] Lide DR. CRC handbook of chemistry and physics. 85th. Boca Raton, FL: CRC Press; 2005.
[47] Bilbao-Sainz C, Sinrod AJG, Williams T, Wood D, Sen Chiou B, Bridges DF, et al. Preservation of tilapia (Oreochromis aureus) fillet by isochoric (constant volume) freezing. J Aquat Food Prod Technol 2020;29:629–40. https://doi.org/10.1080/10498850.2020.1785602.
[48] Phimolsiripol Y, Siripatrawan U, Tulyathan V, Cleland DJ. Effects of freezing and temperature fluctuations during frozen storage on frozen dough and bread quality. J Food Eng 2008;84:48–56. https://doi.org/10.1016/j.jfoodeng.2007.04.016.
[49] Nie B, Palacios A, Zou B, Liu J, Zhang T, Li Y. Review on phase change materials for cold thermal energy storage applications. Renew Sustain Energy Rev 2020;134:110340. https://doi.org/10.1016/j.rser.2020. 110340.
[50] Anisur MR, Mahfuz MH, Kibria MA, Saidur R, Metselaar IHSC, Mahlia TMI. Curbing global warming with phase change materials for energy storage. Renew Sustain Energy Rev 2013;18:23–30. https://doi.org/10.1016/j.rser.2012.10.014.
[51] Wunsch NG. U.S. Frozen foods market - statistics & facts. https://www.statista.com/topics/1339/frozen-foods-market/. [Accessed 1 February 2021].
[52] Research and Markets. Global market study on frozen food: frozen ready meals to be the largest segment by 2020. https://www.businesswire.com/news/home/20150709006092/en/Research-Markets-Global-Market-Study-Frozen-Food. [Accessed 6 February 2021].